J. Biochem. **140**, 237–246 (2006)
doi:10.1093/jb/mvj143

Effect of N-Terminal Region of eIF4E and Ser65-Phosphorylation of 4E-BP1 on Interaction between eIF4E and 4E-BP1 Fragment Peptide

Koji Tomoo[1], Fumi Abiko[1], Hiroo Miyagawa[2], Kunihiro Kitamura[2] and Toshimasa Ishida[1,*]

[1]Department of Physical Chemistry, Osaka University of Pharmaceutical Sciences, 4-20-1 Nasahara, Takatsuki, Osaka 569-1094; and [2]Research Center, Taisho Pharmaceutical Co., Ltd., 1-403 Yoshino-cho, Kita-ku, Saitama 331-9530

Received May 26, 2006; accepted June 13, 2006

To clarify the contribution of N-terminal region of eukaryotic initiation factor 4E (eIF4E) to the interaction with 4E-BP and to investigate the effect of 4E-BP phosphorylation on the interaction with eIF4E, the interaction profiles of the Ser65-unphosphorylated and phosphorylated peptides (Thr37–Thr70 fragment of 4E-BP1) with full-length and N-terminal 33 residues–deleted eIF4Es were investigated by fluorescence and SPR methods. The effect of N-terminal region of eIF4E on the interaction with 4E-BP1 peptides was shown to be dependent on the interaction state, that is, the steady-state fluorescence and kinetic-state SRP analyses showed the positive and negative contributions of the N-terminal region to the interaction with the peptide, respectively, despite its unphosphorylated or phosphorylated state. The comparison of the association constants of the peptide with those of full-length 4E-BP1 indicated the importance of N-terminal (1–36) and/or C-terminal (71–118) sequence of 4E-BP1 for the interaction, although the MD simulations suggested that the α-helical region (Arg56–Cys62) of 4E-BP1 peptide is sufficient for keeping the interaction. The MD simulations also indicated that a charge-dependent rigid hydration shell formed around the phosphate group makes the molecular conformation rigid, and single Ser65 phosphorylation is insufficient for releasing 4E-PB1 peptide from eIF4E.

Key words: 4E binding protein, initiation factor 4E, molecular association, Ser65 phosphorylation.

Abbreviations: eIF4E, eukaryotic initiation factor 4E; d33eIF4E, N-terminal 33 residues–deleted eIF4E; 4E-BP1, eIF4E-binding protein 1; pSer4E-BP1, Ser65-phosphorylated 4E-BP1; MD, molecular dynamics; m^7GTP, 7-methylguanosine-5′-triphosphate; m^7GpppA, P^1–7-methylguanosine-P^3-adenosine-5′,5′-triphosphate; mRNA, messenger RNA; SPR, surface plasmon resonance.

The eukaryotic mRNA has a common cap structure at the 5′-terminal. Eukaryotic initiation factor 4E (eIF4E), which recognizes this cap structure selectively, is a master switch that controls eukaryotic translation of mRNA through the initiation of translation by binding to the cap structure and is regulated by the endogenous 4E-binding protein (4E-BP), where the function of eIF4E is suppressed by the association of 4E-BP and enhanced by dissociation owing to 4E-BP phosphorylation (*1*, *2*). However, the on/off regulation mechanism is still far from the full understanding.

To investigate the structural function of 4E-BP for eIF4E regulation, recently we determined the X-ray crystal structure of the m^7GpppA-bound eIF4E–4E-BP1 peptide (Thr37–Thr70) complex, where m^7GpppA was used as a model compound of the mRNA cap structure, and clarified the interaction mode of the Pro47–Pro66 moiety of the peptide at the binding pocket of eIF4E at the atomic level (Fig. 1A) (*3*). Although the full-length eIF4E was used in this study, the N-terminal 26 residues were not observed in the crystal structure because of their high flexibility. However, the importance of this N-terminal region for the association with eIF4G, a molecular mimic of 4E-BP, was recently reported (*4*). On the other hand, it is known that 4E-BP consists of three isoforms (4E-BP1, 2 and 3) (*5*) with similar binding modes for eIF4E (*3*) and is phosphorylated *in vivo* on multiple residues (*6*, *7*), and 4E-BP binding to eIF4E is reversible and is dependent on the phosphorylation state of 4E-BP. However, concerning the on/off regulation of translation initiation of eIF4E *via* 4E-BP dephosphorylation/phosphorylation, the relationship between the multiple phosphorylation state of 4E-BP and its dissociation from eIF4E remains obscure. For an example, it is unclear why hypophosphorylated 4E-BP isoforms interact strongly with eIF4E, whereas hyperphosphorylated isoforms do not (*8*). Therefore, the study on the structural response of each phosphorylation event regarding the interaction of 4E-BP with eIF4E is important for understanding the regulation mechanism in the initiation step of protein biosynthesis.

Under these backgrounds, it appears important to examine the effect of N-terminal region of eIF4E on the interaction with 4E-BP1 and the structural impact of the single

*To whom correspondence should be addressed. Tel/Fax: +81-726-90-1068, E-mail: ishida@gly.oups.ac.jp

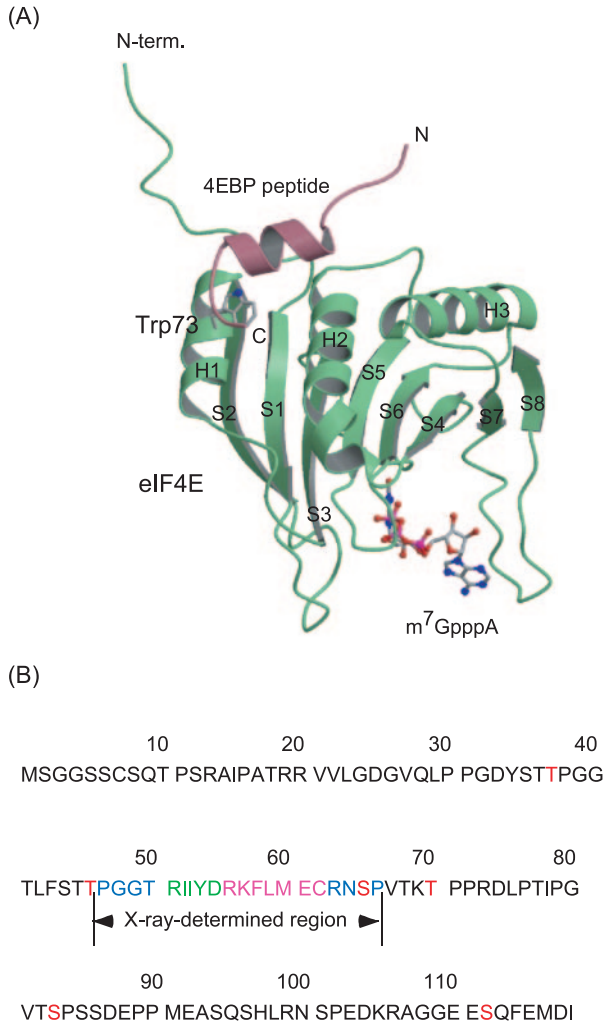

Fig. 1. **(A) X-Ray–determined overall structure of 4E-BP1 Pro47–Pro66 fragment (red ribbon and wire)–eIF4E (green ribbons and wire)–m^7 GpppA (ball and stick) ternary complex and (B) amino acid sequence of full-length human 4E-BP1.** (A) The N-terminal extended (His37–Gln40, green wire) region and H1 (Trp73–Asn77) and H2 (Glu132–Gly139) helical regions (green ribbons) of eIF4E construct 4E-BP1 binding pocket. (B) The phosphorylation residues of 4E-BP1 are marked by red. The Pro47–Pro66 fragment observed in the crystal structure adopted the consecutive extend (Pro47–The50 and Arg63–Pro66, shown by blue), β-sheet (Arg51–Asp55, green), and α-helical (Arg56–Cys62, pink) conformations.

Ser65 phosphorylation of the 4E-BP1 peptide for the interaction with eIF4E; it has been reported that the phosphorylation of Ser65 residue is most influential for binding with eIF4E among multiple Ser and Thr phosphorylation residues of 4E-BP (*9*, *10*), probably due to its hydrogen bond formation with Asn77 at the binding pocket of eIF4E (*3*), although some controversial papers have been reported concerning the possibility of single Ser65 phosphorylation (*11*, *12*). Therefore, we investigated the effect of Ser65 phosphorylation of 4E-BP1 peptide (Thr37–Thr70) on the interaction with full-length and N-terminal 33 residues–deleted eIF4Es bound with m^{7}GTP by the fluorescence and surface plasmon resonance (SPR) methods. By taking advantage of the X-ray–determined atomic coordinates of the m^{7}GpppA-bound eIF4E (Glu27–Val217)–4E-BP1 peptide (Pro47–Pro66) complex (*3*), we also performed molecular dynamics (MD) simulations for the aqueous solution systems of Ser65-unphosphorylated and -phosphorylated 4E-BP1 peptides (Pro47–Pro66), in order to clarify the structural responce for the effect of the phosphorylation of 4E-BP1 on the interaction with the eIF4E. In this paper, we report these results. Perspective binding mode of Pro47–Pro66 fragment of human 4E-BP1 in the binding pocket of human eIF4E, elucidated by X-ray analysis (*3*), is shown in Fig. 1A, and the amino acid sequence of full-length 4E-BP1 protein is shown in Fig. 1B.

MATERIALS AND METHODS

Materials—The peptide of Thr36–Thr70 sequence of human 4E-BP1 (4E-BP1 peptide, Fig. 1B) and its Ser65-phosphorylated peptide (pSer4E-BP1 peptide) were synthesized by Sigma (USA), from which synthetic details can be obtained upon request. The respective peptides obtained in the lyophilized form were characterized by mass spectrometry and determined to be >95.0% pure by reverse-phase HPLC. Recombinant full-length 4E-BP1 was prepared according to a previous method (*3*). Because of the synthetic difficulty, the single Ser65-phosphorylated form of full-length 4E-BP1 was not available in this study.

Recombinant human full-length eIF4E was prepared according to a previous method (*13*). The N-terminal 33 residues–deleted eIF4E (d33eIF4E) gene mutant was prepared by PCR and verified using forward and reverse dideoxy sequencing. The supernatant containing the recombinant protein was applied to the m^{7}GTP-Sepharose 4B affinity column equilibrated with buffer A (20 mM HEPES-KOH, pH 7.5, 1 mM DTT, 0.1 mM EDTA, 100 mM KCl). The preparation of m^{7}GTP-bound eIF4E/d33eIF4E was performed by elution with buffer B (buffer A + 100 μM m^{7}GTP). The sample solutions were concentrated with a Centricon 10 (Amicon Co.) to the desired concentration, which was determined by the Bradford method. The purity of the sample was confirmed by SDS-PAGE.

Fluorescence Spectroscopy—Fluorescence emission spectra were measured on a JASCO FP-6500 with a 10-mm cell. The 300–400 nm measurements were performed at 25°C, where the excitation was fixed at 295 nm. The sample solutions of m^{7}GTP-bound eIF4E/d33eIF4E and of 4E-BP1/pSer4E-BP1 peptides and full-length 4E-BP1 were adjusted using buffer C (10 mM HEPES-NaOH, pH 7.5, 225 mM NaCl, 3 mM EDTA, 0.01% surfactant P20). The intensity change of Trp fluorescence at a 1 μM concentration of eIF4E/d33eIF4E was measured as a function of 4E-BP1/pSer4E-BP1 peptide or full-length 4E-BP1 concentration (0–1.0 μM, in increments of 0.2 μM); the fluorescence of 4E-BP1/pSer4E-BP1 peptide or full-length 4E-BP1 was hardly observed by the excitation at 295 nm. The apparent association constant (K_a) between 4E-BP1 peptide and eIF4E was estimated from the slope of the following equation by least squares linear analysis:

$$Ka = \frac{[eIF4E\text{–}4E\text{–}BP1]}{[eIF4E][4E\text{–}BP1]}$$

$$\frac{F_{eIF4E\text{–}4E\text{–}BP1}}{F_{eIF4E}} = \frac{|\Delta F|}{F} = Ka \cdot [4E\text{–}BP],$$

where $|\Delta F|$ is the absolute value of increased or decreased fluorescence intensity of m^7GpppA-bound eIF4E by the interaction with 4E-BP1 peptide; the K_a values for other combinations were also obtained by the same manner. The experiments were at least three times performed, and the K_a values were averaged.

SPR Measurement—A binding assay was performed using BIAcore X (Biacore, Inc., Uppsala, Sweden), according to a previous method (*14*). A sensor chip, which was prepared from a dextran-coated chip (Sensorchip CM5, Biacore) in the conventional manner, was immobilized by the injection of 4E-BP1/pSer4E-BP1 peptide or full-length 4E-BP1 in buffer C (final concentration = 100 μg/ml) and then m^7GTP-bound eIF4E/d33eIF4E was eluted as a function of the concentration range of 9–625 nM. The chip was regenerated after each cycle using 10 mM glycine-HCl buffer (pH 2.2). All measurements were performed at a flow rate of 20 μl/min at 25°C. The obtained sensorgrams were evaluated using the BIA evaluation software package, by which the responses from the inactivated dextran-coated chips measured as a reference were subtracted from the sample responses to obtain the sensorgram for a specific interaction. The rate constants for association, k_a, and dissociation, k_d, and the equilibrium constant for association, K_A (= k_a/k_d), were obtained using global fittings for Langmuir binding; the respective values were checked for consistency using local fitting. The experiments were at least three times performed, and the values were averaged.

Molecular Dynamics Simulation—X-ray crystal structure of 4E-BP1 peptide (Thr36–Thr70) in the complex with m^7GpppA-bound full-length eIF4E (*3*) determined the atomic positions of Pro47–Pro66 moiety for 4E-BP1 peptide and of Glu27–Val217 moiety for eIF4E, and the remaining parts of 4E-BP1 peptide and eIF4E (Met1–Gln26) were not determined due to their high thermal motions. Therefore, the MD simulations were performed for two aqueous solution systems of 4E-BP1 and pSer4E-BP1 peptides (Pro47–Pro66) in the complex with m^7GpppA-bound and N-terminal 26 residues–deleted eIF4E (Glu27–Val217). The atomic coordinate of phosphorylated Ser65 was constructed manually on a graphics computer. The simulations were performed assuming a neutral pH of 7.0, where the phosphate group was treated in dianionic form. To neutralize the system, chloride ions were included. Each solute (eIF4E, 4E-BP1/pSer4E-BP1 peptide, chloride ions) was then placed in a rectangular box ($65 \times 75 \times 72$ Å^3) filled with TIP3P water molecules (*15*); the total number of atoms was about 29,000 for the respective systems. An AMBER all-atom force field (*16*) was used for the solute.

The MD simulations were performed by using the AMBER 6 program (*17*), where the periodic boundary condition was used, and the electrostatic interaction was calculated using the Particle–Meshed–Ewald method (*18*). Using the Berendsen algorithm (*19*) with a coupling time of 0.2 ps, temperature and pressure were controlled at 300 K and 1 atm, respectively. The simulation of each system was performed according to the protocol described in a previous paper (*3*), where the SHAKE (*20*) constraints were applied for hydrogen atoms. After the initial relaxation procedure for 1,300 ps, the MD simulations reached the stationary states within 50 ps, as determined from their fluctuations within ±3% with respect to the respective potential energies. Ser65 phosphorylation stabilized the average total potential energy by approximately 1,400 kcal/mol: –92,300 ± 200 kcal/mol for the unphosphorylated system and –93,750 ± 200 kcal/mol for the phosphorylated system.

RESULTS

Fluorescence Analyses—The X-ray crystal analysis of m^7GpppA-bound eIF4E–4E-BP1 peptide complex (*3*) clarified the interaction of Trp73 residue of eIF4E with 4E-BP1 peptide, and suggested that the fluorescence of this Trp residue could be used as a probe for the interaction of eIF4E and 4E-BP1 peptide (see Fig. 1A). To investigate the effects of N-terminal region of eIF4E and Ser65-phosphorylation of 4E-BP1 peptide on the interaction of both molecules, therefore, the steady-state fluorescence emission spectra of m^7GTP-bound full-length eIF4E and its N-terminal 33 residues–deleted eIF4E (d33eIF4E) were measured as a function of 4E-BP1/pSer4E-BP1 peptide concentration at 25°C (Fig. 2A). The plots of $|\Delta F|$–4E-BP1/pSer4E-BP1 concentration are shown in Fig. 2B, and the apparent association constants are given in Table 1a. The spectral behavior of eIF4E fluorescence was different in the interactions with the Ser65-unphosphorylated and -phosphorylated 4E-BP1 peptides. Whereas the fluorescence intensity of eIF4E increased proportionally with the concentration of unphosphorylated peptide, the phosphorylation induced the quenching of fluorescence intensity. This indicates that the binding modes of both peptides at the pocket of eIF-4E are different from each other. Similar increased intensity or quenching of eIF4E fluorescence was reported in the interaction with human full-length 4E-BP1 (*3*) or its fragment peptide (amino acid sequence of 51–67) (*21*), respectively. The increase of fluorescence intensity would result from the decreased flexibility of Trp indole ring, while the quenching would be due to the Trp residue buried in the hydrophobic situation. Another feature of emission spectra is the blue shift of fluorescence peak by the addition of 4E-BP1 or pSer4E-BP1 peptide. This would reflect the decreased π-electron resonance of Trp indole ring with the neighboring acceptor group. On the basis of these spectral features, therefore, it would be considered that the Trp indole ring is fixed on the molecular surface by the interaction with the 4E-BP1 peptide, whereas the Trp residue is buried into the hydrophobic space of eIF4E by the interaction, in which no specific stacking interaction is formed.

The plots of $|\Delta F|$–4E-BP1/pSer4E-BP1 concentration showed the 1:1 stoichiometric bindings for all interaction pairs between 4E-BP1/pSer4E-BP1 peptides and m^7GTP-bound eIF4E/d33eIF4E (Fig. 2B). The fluorescence intensity was little changed at above 1 μM concentration of 4E-BP1 or pSer4E-BP1 peptide, and this indicates that no more than one 4E-BP molecule is necessary to completely occupy the 4E-BP–binding pocket of eIF4E.

The apparent association constants given in Table 1a show that (i) the Ser65-phosphorylation strengthens to some extent the interaction between 4E-BP1 peptide and eIF4E, meaning that the single phosphorylation of Ser65 is insufficient for releasing 4E-BP1 peptide from eIF4E and (ii) the N-terminal flexible region of eIF4E plays a role in

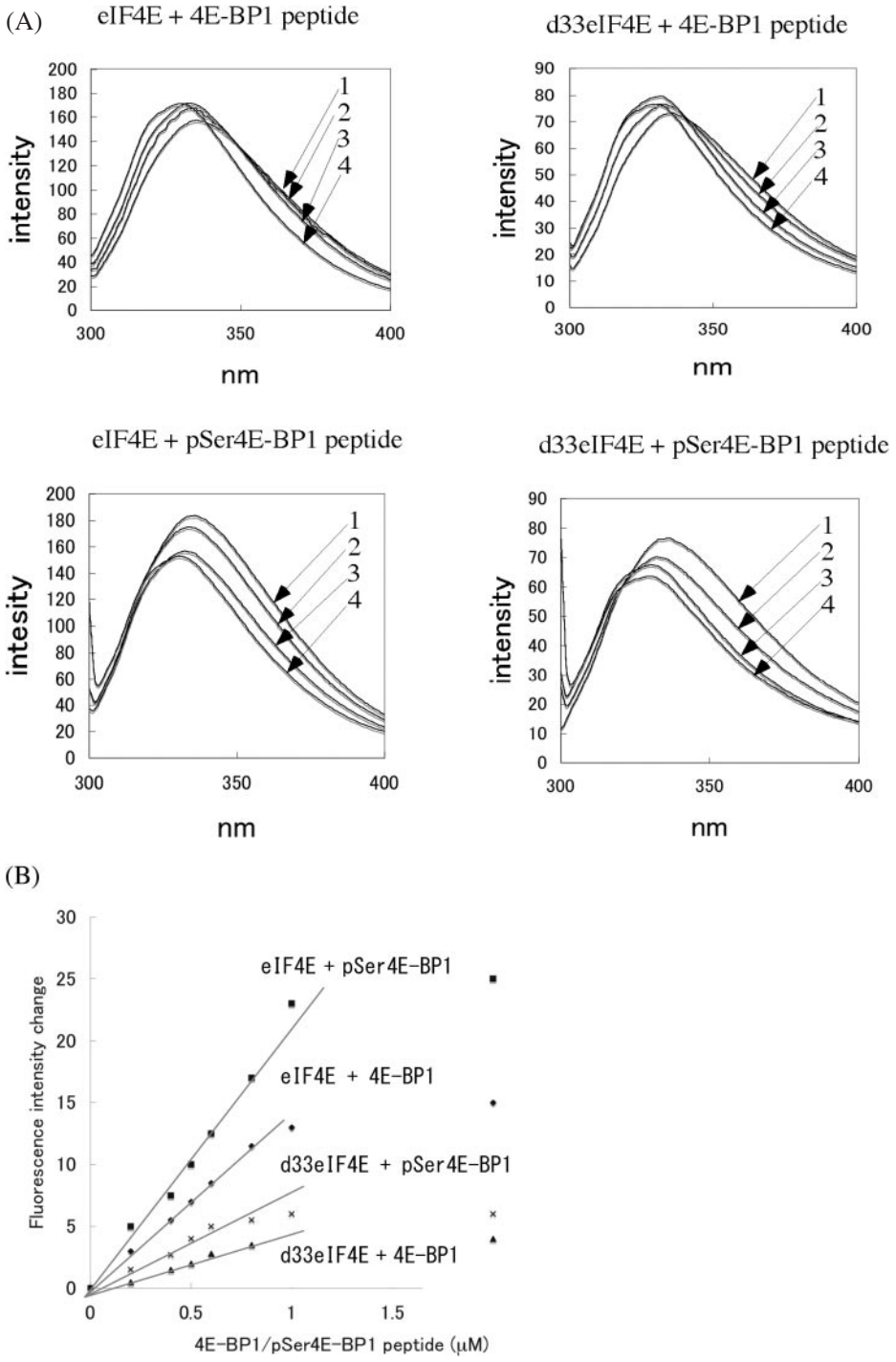

Fig. 2. **(A) Fluorescence emission spectral change of m^{7}GTP-bound eIF4E or d33eIF4E (1 μM) in different 4E-BP1 or pSer4E-BP1 peptide concentration and (B) plot of fluorescence intensity change (absolute value) at a maximum peak as a function of 4E-BP1 or pSer4E-BP1 concentration.** (A) The concentration of 4E-BP1/pSer4E-BP1 peptide corresponds to 1: 0 μM, 2: 0.5 μM, 3: 1.0 μM and 4: 5.0 μM. (B) The respective lines and slopes were obtained by the least-squares fits of the observed data of 0–1 μM 4E-BP1/pSer4E-BP1 peptide concentration.

increasing the interaction with 4E-BP1 despite the unphosphorylated/phosphorylated Ser65.

On the other hand, the association constants of full-length 4E-BP1 showed about one to two order of magnitude larger than those of the peptide, indicating the importance of N-terminal (1–36) and/or C-terminal (71–118) sequence of 4E-BP1 for the interaction, and its effect was much more significant for the interaction with eIF4E than d33eIF4E. Previously, we reported the 3:2 stoichiometry for the interaction between m^{7}GpppA-bound eIF4E and 4E-BP1 (*3*).

Table 1. Binding data of 4E-BP1/pSer4E-BP1 with m^7 GTP-bound eIF4E/d33eIF4E.

(a) Apparent association constants by the fluorescence method at 25°C.

	K_a (1/M)/10^6
eIF4E+ 4E-BP1 peptide	18 ± 2
d33eIF4E + 4E-BP1 peptide	6 ± 2
eIF4E + pSer4E-BP1 peptide	25 ± 2
d33eIF4E + pSer4E-BP1 peptide	10 ± 2
	K_a (1/M)/10^7
eIF4E + 4E-BP1 full length	67 ± 3
d33eIF4E + 4E-BP1 full length	15 ± 3

(b) Binding parameters by the SPR method at 25°C.

	k_a (1/M·s)/10^5	k_d (1/s)/10^{-2}	K_A (1/M)/10^6
eIF4E + 4E-BP1 peptide	2.2 ± 0.3	9.8 ± 0.2	2.2 ± 0.6
d33eIF4E + 4E-BP1 peptide	3.8 ± 0.4	2.1 ± 0.1	18.6 ± 3.1
eIF4E + pSer4E-BP1 peptide	2.1 ± 0.3	19.6 ± 0.3	1.1 ± 1.2
d33eIF4E + pSer4E-BP1 peptide	4.5 ± 0.4	5.5 ± 0.1	8.2 ± 0.9
	k_a (1/M·s)/10^5	k_d (1/s)/10^{-3}	K_A (1/M)/10^8
eIF4E + 4E-BP1 full length	3.7 ± 0.5	7.8 ± 0.8	0.5 ± 0.1
d33eIF4E + 4E-BP1 full length	7.2 ± 0.8	0.4 ± 0.2	24 ± 14

The difference from the present 1:1 stoichiometric binding may be due to the presence of this N- and/or C-terminal deleted sequence of 4E-BP1.

SPR Analyses—To further quantitatively investigate the structural function of eIF4E N-terminal 33 residues for the interaction and the effect of Ser65-phosphorylation of 4E-BP1 on the interaction with eIF4E, the SPR analyses were performed for four different pairs. The binding curves were monitored as a function of the reaction time by SPR signals, and the results are shown in Fig. 3. The k_a, k_d, and K_A values, obtained by respective SPR analyses, are summarized in Table 1b.

Despite the unphosphorylated/phosphorylated 4E-BP1 peptide, the SPR profiles (Fig. 3) clearly showed the fast association and dissociation rates of N-terminal deleted eIF4E, compared with those of the full-length eIF4E. This is reflected by the increased k_a and decreased k_d values of d33eIF4E, compared with those of full-length eIF4E. Thus, this characteristic may indicate the function of N-terminal region of eIF4E as the repressor for the association/dissociation reaction with 4E-BP. It is obvious from the K_A values in Table 1b that (i) the Ser65-phosphorylation weakens the interaction of 4E-BP1 peptide with eIF4E and (ii) both the 4E-BP1 and pSer4E-BP1 peptides commonly increase the interaction with eIF4E by the deletion of its N-terminal 33 residues. These results are just opposite from those by the fluorescence method. Although both methods quantify the bound fraction of the peptide, their way to estimate the bound fraction is different, *i.e.*, the fluorescence measures the interaction in a steady equilibrium state, while the SPR measurement is performed at a kinetic state under a definite flow rate of the pair. Thus, it could say that the contribution of N-terminal region of eIF4E to the interaction is dependent on the interaction state of both molecules.

The importance of N-terminal (1–36) and/or C-terminal (71–118) sequence of 4E-BP1 for the interaction was again shown from the SPR binding parameters in Table 1b. The K_A values of full-length 4E-BP1 showed about two orders of magnitude larger than those of the peptide. Interestingly, the inhibitory effect of N-terminal region of eIF4E on the molecular interaction is significantly increased in the presence of these N- and/or C-terminal sequence of 4E-BP1, where the interaction of both molecules is about 36-fold strengthened by the lack of N-terminal region of eIF4E.

MD Simulations—To clarify the structural basis for the interaction of eIF4E with 4E-BP1 peptide and the structural responce of phosphorylation to the interaction, the MD simulations were performed for the 4E-BP1 and pSer4E-BP1 peptides (Pro44–Pro66) in the complex with m^7GpppA-bound and N-terminal 26 residues-deleted eIF4E (Glu27–Val217).

Electronic State–Dependent Hydrogen Bonding Water Shell Formation by Phosphorylation—It is noteworthy that a large and rigid hydrogen bonding water shell is created by the interaction of phosphate oxygen atoms with the surrounding water molecules in an aqueous solution, where the size of the hydrogen bonding shell is dependent on the electronic state of the phosphate group, that is, monoanionic or dianionic state. As is shown in Table 2a, MD simulation during 5ns showed that the total number of water molecules, which form hydrogen bonds or short contacts with the phosphate oxygen atoms, considerably differs between the monoanionic and dianionic states: on average, about ten water molecules form a rigid hydrogen bonding shell around a dianionic phosphate group within a O . . . O distance of 2.9 Å, whereas five water molecules are on average bound to a monoanionic phosphate group. These hydrogen bonding water molecules are spherically fixed around the phosphate group and distinguishable from the other freely movable water molecules, because most of these water molecules synchronize with the dynamic movement of the phosphate group. As a definite spatial space is required around the phosphate group to form such a hydration shell, the dianionic phosphorylation would cause a large structural change, compared with monoanionic phosphorylation, and this may be one of the major factors for the phosphorylation-mediated structural change that enables the signal transmission between biomolecules.

Importance of α-Helical Moiety of 4E-BP1 Peptide for Interaction with eIF4E—The MD simulation of the pSer4E-BP1 peptide was performed assuming a dianionic state, because the pK_2 of the phosphate group in the related biomolecules is in the range of 5 to 7 and the biological function of 4E-BP is active at a neutral pH. To investigate the effect of Ser65 phosphorylation on the interaction with eIF4E, the time–distance profiles of some selected 4E-BP1–eIF4E atomic pairs were compared between the unphospholylated and phosphorylated peptides (Fig. 4), and the average distances and deviations of the atomic pairs that directly connected both molecules

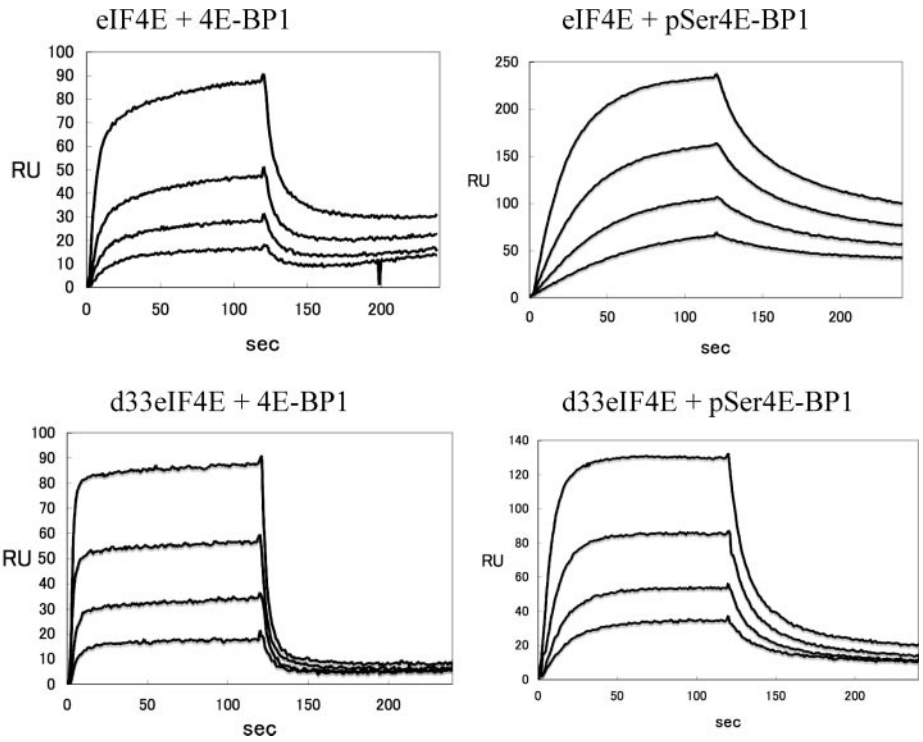

Fig. 3. **SPR sensorgrams of 4E-BP1 or pSer4E-BP1 peptide as a function of m^7GTP-bound eIF4E/d33eIF4E concentration.** Each SPR signal reflects the time response of the addition of m^7GTP-bound eIF4E/d33eIF4E to the CM5-coated chip bearing the 4E-BP1/pSer4E-BP1 peptide (~500 RU). The right and left parts of each sensorgram indicate the phases of binding (injection of m^7GTP-bound eIF4E/d33eIF4E) and of release (exposure of the chip to eIF4E/d33eIF4E-free buffer), respectively. The concentration of eIF4E/d33eIF4E corresponds to 19, 39, 78, 156 and 312 nM for eIF4E–4E-BP1, 9, 19, 39, and 78 nM for eIF4E–pSer4E-BP1, 78, 156, 312, 625 nM for d33eIF4E–4E-BP1 and 19, 39, 78 and 156 nM for d33eIF4E–pSer4E-BP1 in an increasing RU order at 100 s.

Table 2. MD simulation data of water shell formation by Ser65-phosphorylation and molecular interaction of 4E-BP1/pSer4E-BP1 peptide–m^7 GpppA-bound eIF4E complexes.

(a) Average numbers of water molecules surrounding mono or dianionic phosphate group of pSer4E-BP1.

	⩽2.7 Å	⩽2.9Å	⩽3.1Å	⩽3.3Å
Monoanionic	1 ± 1	5 ± 2	8 ± 3	12 ± 3
Dianionic	5 ± 2	10 ± 2	12 ± 2	14 ± 2

(b) Intermolecular hydrogen bonds or short contacts between 4E-BP1 or pSer4E-BP1 and eIF4E.

4E-BP1/ pSer4E-BP1	eIF4E	MD simulation range	Distance (Å)	
			4E-BP1	pSer4E-BP1
Tyr54 $O^{\eta}H$	Pro38 O	0–5 ns	2.73 ± 0.17	2.71 ± 0.12
Arg56 $N^{\varepsilon}H$	Glu132 $O^{\varepsilon 1}$	0–5 ns	3.03 ± 0.29	2.97 ± 0.21
Arg56 $N^{\eta 2}H$	Glu132 $O^{\varepsilon 2}$	0–5 ns	2.87 ± 0.29	2.83 ± 0.20
Leu59 O	Trp73 $N^{\varepsilon 1}H$	0–5 ns	2.96 ± 0.20	2.91 ± 0.16
Arg51 $N^{\eta 1}H$	Glu32 $O^{\varepsilon 2}$	2.5–5 ns	2.99 ± 0.32	
Arg51 $N^{\eta 2}H$	Glu32 $O^{\varepsilon 1}$	2.5–5 ns	2.95 ± 0.36	
Pro47 O	Ser146 NH	2.5–5 ns		3.64 ± 0.85
Pro47 O	Asp147 NH	2.5–5 ns		3.42 ± 0.79
Arg51 $N^{\varepsilon}H$	Gln40 $O^{\varepsilon 1}$	3.5–5 ns		3.32 ± 0.61
Glu61 O	His33 $C^{\varepsilon 1}$	4–5 ns		3.32 ± 0.33
Asn64 $N^{\delta 2}H$	His33 O	2.5–5 ns		3.23 ± 0.49
Asn64 $O^{\delta 1}$	Lys36 $N^{\eta}H$	4–5 ns		3.62 ± 1.15
pSer65 PO^3	Lys36 $H^{\eta}H$	4–5 ns		3.37 ± 0.80
Phe58 C^Z	His37 C^{ε}	0–5ns	5.17 ± 1.02	4.48 ± 0.45
Met60 S^{γ}	Leu135 C^{δ}	0–5ns	5.55 ± 1.20	4.76 ± 0.67
Cys62 C^{β}	Val69 $C^{\delta 1}$	0–5ns	5.67 ± 1.39	3.91 ± 0.60

through the hydrogen bonds or short contacts are shown in Table 2b. The modes of the binding of 4E-BP1 and pSer4E-PB1 peptides to eIF4E at the stage of 5 ns MD simulation are shown in Fig. 5.

The present MD simulation showed that (i) the single phosphorylation of Ser65 does not release the 4E-BP1 peptide from eIF4E; this agrees with the present spectral result, and (ii) the stable docking of 4E-BP1 peptide in

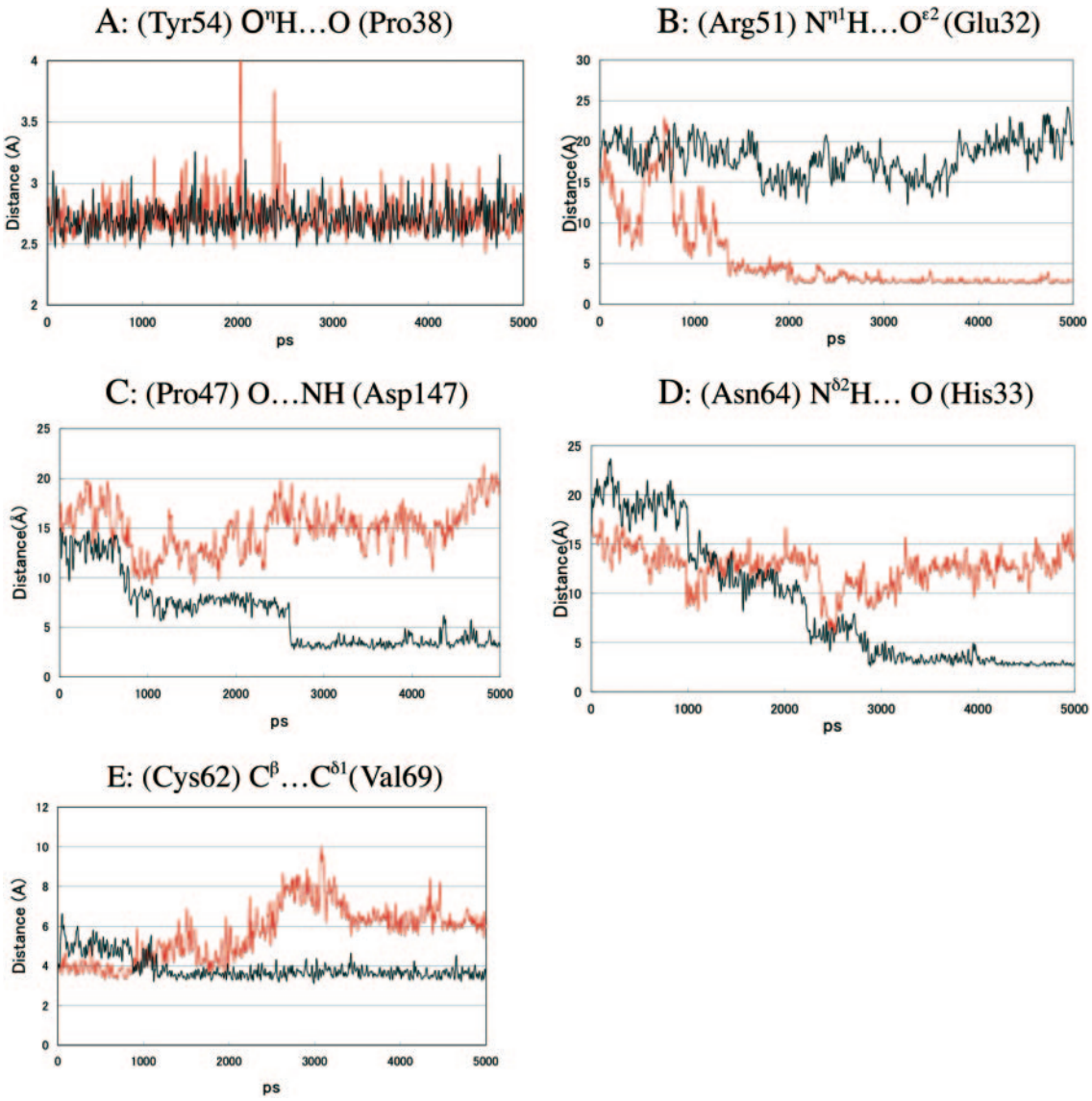

Fig. 4. **Time profiles of selected 4E-BP1/pSer4E-BP1 . . . eIF4E atomic pairs.** The red and black lines represent the profiles of 4E-BP1 . . . eIF4E and pSer4E-BP1 . . . eIF4E atomic pairs, respectively.

the pocket of eIF4E is due to four hydrogen bonds of (Tyr54)O$^{\eta}$H . . . O(Pro38), (Arg56)N$^{\varepsilon}$H . . . O$^{\varepsilon 1}$(Glu132), (Arg56)N$^{\eta 2}$H . . . O$^{\varepsilon 2}$(Glu132), and (Lye59)O . . . H$^{\varepsilon}$N(Trp73); N(Trp73); their interatomic distances were maintained within the hydrogen bonding distance throughout the MD simulations without any large bond break in both the 4E-BP1 and pSer4E-BP1 complexes (for example, see Fig. 4A).

It is remarkable to note that these hydrogen-bonding residues are all close to or in the α-helical region of 4E-BP1 peptide (see Fig. 1B). As is obvious from Table 3a, the conformation of helical moiety (from Arg56 to Met61) is rigid and is hardly affected by the Ser65 phosphorylation, compared with those of other moieties, indicating the importance of the α-helical structure of 4E-BP1 peptide for the stable binding with eIF4E.

Effects of Phosphorylation on Conformation of 4E-BP1 Peptide and Interaction with eIF4E—The MD conformational trajectory of 4E-BP1 peptide was considerably different from that of the pSer4E-BP1 peptide. As can be estimated from Table 3b and Fig. 5, the 4E-BP1 peptide was subjected to the intramolecularly controlled conformational trajectory without receiving any specific restraint from the binding pocket of eIF4E, except for the above-mentioned four hydrogen bonds at the central sheet and α-helical moieties. Only a pair of hydrogen bonds was formed between Arg51(4E-BP1) and Glu32(eIF4E) residues for the 2.5–5 ns MD simulation (Table 2b and Fig. 4B). The N-terminal Pro-Gly-Gly sequence deviated markedly from the MD-starting X-ray structure to approach the C-terminal region, thus transforming a round conformation of whole peptide with a relatively large fluctuation (Table 3b). In contrast, the pSer4E-BP1 peptide formed more hydrogen bonds or short contacts than 4E-BP1 during the MD simulation of 5 ns (Table 2b). The N-terminal Pro47 O atom formed a bifurcated interaction with NHs of Ser146 and Asp147 of eIF4E at

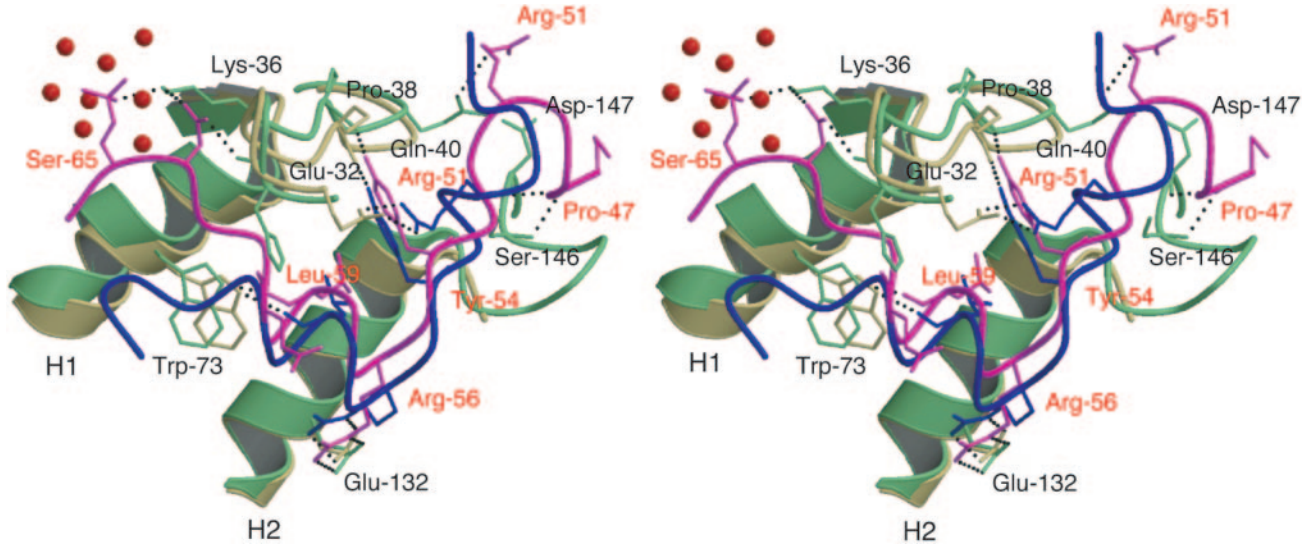

Fig. 5. **Stereoscopic views of superimposed binding modes of 4E-BP1 (blue wire and stick) and pSer4E-BP1 peptides (magenta wire and stick) in binding pocket of eIF4E (green ribbons and wire for pSer4E-BP1 complex and khaki ribbons and wire for 4E-BP1 complex) at 5 ns MD simulation.** The hydrogen bonds are shown as dotted lines. The red circles represent water molecules located around the Ser65 phosphate group within 2.9 Å. Some functional residues are shown as stick bonds with red residual names for 4E-BP1/pSer4E-BP1 and black ones for eIF4E.

Table 3. MD data of molecular conformation of 4E-BP1/pSer4E-BP1 peptide.

(a) Standard deviations of ϕ and ψ torsion angles (°) of some selected residues of 4E-BP1/pSer4E-BP1 peptide from their averaged values.

Residue	Secondary structural region[a]	4E-BP1		pSer4E-BP1	
		ϕ	ψ	ϕ	ψ
Gly49	N-extend	34	25	31	34
Arg51	sheet	25	18	36	15
Ile52	sheet	20	24	16	15
Tyr54	sheet	28	56	31	73
Arg56	helix	10	11	8	9
Leu59	helix	9	14	8	9
Arg63	C-extend	62	94	83	42
Ser65	C-extend	13	11	81	47

(b) Average distances and their deviations for selected Cα–Cαdistances within 4E-BP1/pSer4E-BP1 peptides.

	Atomic pair	Secondary structural region	4E-BP1	pSer4E-BP1
Pro47	Pro66	N-extend–C-extend	31 ± 2 Å	35 ± 1 Å
Pro47	Asp55	N-extend–sheet	15 ± 3	18 ± 1
Pro47	Cys62	N-extend–helix	22 ± 2	26 ± 1
Arg51	Cys62	sheet–helix	14 ± 1	18 ± 1
Arg56	Pro66	helix–C-extend	17 ± 2	13.3 ± 0.7 (0–1 ns)
				21.2 ± 0.6 (3–5ns)

[a]N- and C-extends represent the N- and C-terminal extended regions, respectively.

about 2.5 ns and maintained the interaction (Fig. 4C), and the C-terminal Asn64 amide group approached the His33 O of eIF4E as the MD simulation processed and formed the short contacts including the hydrogen bonds at about 4 ns (Fig. 4D). Characteristically, one (PO^3) of three phosphate O atoms of pSer65 formed a short contact with Lys36 $N^{\zeta}H$ of eIF4E during 4–5 ns of MD simulation (Table 2b), contributing to the continued interaction of pSer4E-BP1 with eIF4E. These interactions at both N- and C-terminal regions, in addition to the four intermolecular hydrogen bonds at central sheet and α-helical regions, are the main factors for the decreased conformational fluctuation of the pSer4E-BP1 peptide.

A further marked feature observed in Ser65 phosphorylation is the enhanced hydrophobic interaction between both molecules. The hydrophobic interactions of Phe58(4E-BP1)...His37 (eIF4E), Met60...Trp73/Leu135, and Cys62...His37/Val69 side chains were considerably enhanced by the phosphorylation (Table 2b and Fig. 4E). As these residues are located at the helical region of pSer4E-BP1, we could say that the increased hydrophobic interactions, concerted with four intermolecular hydrogen

bonds, lead to the close contacts between the remaining region of 4E-BP1 peptide and eIF4E. With the increased intermolecular interaction, consequently, pSer4E-BP1 restricts considerably the fluctuation of the overall conformation (Table 3b).

Characteristically, the Arg56 . . . Pro66 pair showed drastic conformational change during 1–1.2 ns after starting MD simulation by the Ser65 phosphorylation (Table 3b). The C-terminal Asn-Ser-Pro sequence of pSer4E-BP1 peptide deviated markedly from its MD-starting X-ray structure to align with the helical direction of Arg56–Arg63, consequently, transforming an extended and less flexible conformation, which is in contrast with the case of 4E-BP1 peptide (Fig. 5).

DISCUSSION

Although 4E-BP regulation in the translation initiation of eIF4E is achieved by the dephosphorylation and phosphorylation of 4E-BP *via* association with and dissociation from eIF4E, respectively, the detailed structural mechanism for this regulation remains to be clarified. For an example, it is unknown the structural scaffold to explain why hypophosphorylated state of 4E-BP1 is still able to associate with eIF4E, whereas its hyperphosphorylation dissociates from eIF4E (*8*). Also, although the flexible N-terminal region of eIF4E has been reported to be important for the association with eIF4G (*4*), a molecular mimic of 4E-BP, the study on its structural function is still very few. To clarify the effect of N-terminal flexible region of eIF4E and of single Ser65 phosphorylation of 4E-BP1 on these molecular interaction, therefore, the fluorescence and SPR spectroscopic analyses were performed for the interactions of the Ser65-phosphorylated 4E-BP1 peptide with full-length and N-terminal 33 residues–deleted eIF4Es and compared with those of the unphospharylated peptide. Furthermore, by taking advantage of X-ray-determined atomic coordinates of the complexes (*3*), the MD simulation during 5 ns was performed to clarify the structural basis for the interaction of eIF4E with 4E-BP1 peptide and the structural response of phosphorylation to the interaction,

As for the effect of the N-terminal region of eIF4E on the association with 4E-BP1 peptide, the fluorescence and SPR analyses showed the opposite contribution, despite the unphosphorylated/phosphorylated state of the peptide, that is, the decreased and increased interactions from the former and latter analyses, respectively. Similarly, concerning the Ser65 phosphorylation of 4E-BP1 peptide, the opposite result was also observed between these methods, that is, the increase and decrease of the interaction by the former and latter analyses, respectively. Probably, this inconsistency would be resulted from the different way to estimate the interaction, *i.e.*, the fluorescence analysis is based on the molecular interaction under a steady equilibrium state, while the SPR measurement is performed at the kinetic interaction state under a definite flow rate of a pair's molecule. On the basis of the present results, therefore, it may say that the N-terminal region of eIF4E functions as a repressor for the association/dissociation reaction with 4E-BP, that is, it acts so as to stabilize the complex in an equilibrium state and to block the docking of 4E-BP1 to the binding pocket of eIF4E in a non-steady kinetic state. On the other hand, the importance of N-terminal (1–36) and/or C-terminal (71–118) sequence of 4E-BP1 for the interaction with eIF4E was shown by the comparison of the association constants of the full-length 4E-BP1 with those of the peptide; this terminal sequence causes more than two orders of magnitude in interaction, the effect of which on the interaction is more significant than that of N-terminal region of eIF4E.

The MD simulations performed for the m^7GpppA-bound and N-terminal 26 residues-deleted eIF4E–4E-BP1 peptide (Pro44–Pro66) complex showed that the structural impact of Ser65 phosphorylation is largely attributable to the electric state of phosphate, and the dianionic form creates a large and rigid hydration water shell around the phosphate group, compared with the monoanionic form. As these hydrated water molecules synchronize with the dynamic movement of the phosphate group, it could be thought that a definite spatial space for hydration is required around the phosphate group, and consequently the phosphorylated Ser65 behaves as a large hydrophilic residue and orients its side chain toward the surrounding aqueous layer to avoid electrostatic repulsion with neighboring residues and to maximize the space for hydration. This would be a main reason why the kinetic-state SPR analysis showed the decreased interaction of 4E-BP1 peptide with eIF4E by the phosphorylation. On the other hand, the formation of such a hydration shell produces a pushing force toward the back region of the phosphate, because the freely movable water molecules, which are pushed aside by the shell formation, continuously react against the pushing action. In the present case, such a force makes 4E-BP1 an open and rigid conformation.

As was already reported by other groups (*21*, *22*), the MD simulation also showed that the single Ser65 phosphorylation does not lead to the dissociation of 4E-BP1 peptide from eIF4E; four hydrogen bonds of Tyr54 $O^{\eta}H \ldots O$ Pro38, Arg56 $N^{\varepsilon}H \ldots$ Glu132 $O^{\varepsilon 2}$, Arg56 $N^{\eta 2}H \ldots$ Glu132 $O^{\varepsilon 2}$, and Leu59 $O \ldots N^{\varepsilon 1}H$ Trp73 atomic pairs played important role in the binding of both molecules. Reversely, the phosphorylation led to enhanced hydrophobic interactions with eIF4E at the α-helical structural moiety of 4E-BP1 peptide. This agrees well with the increased association constant by the 4E-BP1 phosphorylation, observed by the steady-state fluorescence analysis, and explains why the hypophosphorylated 4E-BP1 still interacts with eIF4E, reported by Gingras *et al.* (*8*). Also the increased Met60. . .Trp73 hydrophobic interactions may be a reason why the fluorescence intensity of eIF4E was quenched by the interaction with pSer4E-BP1 peptide.

The MD simulation also showed that the molecular conformation of the unphosphorylated 4E-BP1 peptide is relatively flexible and is transformed into a round form. Because the central helical structure was hardly affected by the phosphorylation, the different conformational trajectory from that of pSer4E-BP1 peptide clearly reflects the difference between 4E-BP1 and pSer4E-PB1 peptides for the interaction with eIF4E. Therefore, the decreased interaction with eIF4E by the 4E-BP1phosphorylation, shown by the SPR analysis, may be resulted from the rigidified conformation of pSer4E-BP1, because it is disadvantageous for the overall interfacial interaction with eIF4E; the enhanced structural rigidity by phosphorylation has

also been reported in other phosphorylation-regulated proteins (*23*).

Concerning the phosphorylation of 4E-BP1, a hierarchical phosphorylation step has been reported (*22*), *i.e.*, phosphorylation of Thr37/Thr46 is followed by Thr70 phosphorylation, and Ser65 is lastly phosphorylated. Also, it has been reported that the phosphorylation of Ser65 is facilitated by the phosphorylations of Thr37, Thr46, and Thr70 (*11*). Thus, the present single Ser65 phosphorylation may not reflect a physiological situation on 4E-BP1 phosphorylation. However, the insights on the conformational and interaction feature of 4E-BP1 peptide by phosphorylation, together with the functions of N-terminal region of eIF4E and of N-terminal and/or C-terminal sequence of 4E-BP1 for the interaction, would be important to understand the regulation mechanism of eIF4E by 4E-BP isoforms.

This work was supported by a Grant-in-Aid for High Technology Research from the Ministry of Education, Science, Sports and Culture, Japan.

REFERENCES

1. Gingras, A.C., Raught, B., and Sonenberg, N. (1999) EIF4 initiation factors: effectors on mRNA recruitment to ribosomes and regulators of translation. *Annu. Rev. Biochem.* **68**, 913–963
2. Sonenberg, N. and Dever, T.E. (2003) Eukaryotic translation initiation factors and regulators. *Curr. Opin. Struct. Biol.* **13**, 56–63
3. Tomoo, K., Matsushita, Y., Fujisaki, H., Abiko, F., Shen, X., Taniguchi, T., Miyagawa, H., Kitamura, K., Miura, K., and Ishida, T. (2005) Structural basis for mRNA cap-binding regulation of eukaryotic initiation factor 4E by 4E-binding protein, studied by spectroscopic, X-ray crystal structural, and molecular dynamics simulation methods. *Biochim. Biophys. Acta* **1753**, 191–208
4. Gross, J.D., Moerke. N.J., Von der Haar, T., Lugovskoy, A.A., Sachs, A.B., McCarthy, J.E.G., and Wagner, G. (2003) Ribosome loading onto the mRNA cap is driven by conformational coupling between eIF4G and eIF4E. *Cell* **115**, 739–750
5. Sonenberg, N. (1996) mRNA 5′cap-binding protein eIF4E and control of cell growth in *Transcriptional Control* (Hershey, J.WB. *et al*., eds.) pp. 245–269, Cold Spring Harbor Laboratory Press, New York
6. Fadden, P., Haystead, T.A., and Lawrence, J.C., Jr. (1997) Identification of phosphorylation sites in the translational regulator, PHAS-1, that are controlled by insulin and rapamycin in rat adipocytes. *J. Biol. Chem.* **272**, 10240–10247
7. Heesom, K.J, Avison, M.B., Diggle, T.A., and Denton, R.M. (1998) Insulin-stimulated kinase from rat fat cells that phosphorylates initiation factor-4E binding protein 1 on the rapamycin-insensitive site [serine-111]. *Biochem. J.* **336**, 39–48
8. Gingras, A.C., Gygi, S.P., Raught, B., Polakiewicz, R.D., Abraham, R.T., Hoekstra, M.F., Aebersold, R., and Sonenberg, N. (1999) Regulation of 4E-BP1 phosphorylation: a novel two-step mechanism. *Genes Dev.* **13**, 1422–1437
9. Karim, M.M., Hughes, J.M.X., Warwicker, J., Scheper, G.C., Proud, C.G., and McCarthy, J.E.G. (2001) A quantitative molecular model for modulation of mammalian translation by the eIF4E-binding protein 1. *J. Biol. Chem.* **276**, 20750–20757
10. Tee, A.R. and Proud, C.G. (2002) Caspase cleavage of initiation factor 4E-binding protein 1 yields a dominant inhibitor of cap-dependent translation and reveals a novel regulatory motif. *Mol. Cell. Biol.* **22**, 1674–1683
11. Mothe-Satney, I., Brunn, G.J., McMahon, L.P., Capaldo, C.T., Abraham, R.T., and Lawrence, J.C., Jr. (2000) Mammalian target of rapamycin-dependent phosphorylation of PHAS-I in four (S/T)P sites detected by phospho-specific antibodies. *J. Biol. Chem.* **275**, 33836–33843
12. McMahon, L.P., Choi, K.M., Lin, T.A., Abraham, R.T., and Lawrence, J.C., Jr. (2002) The rapamycin-binding domain governs substrate selectivity by the mammalian target of rapamycin. *Mol. Cell. Biol.* **22**, 7428–7438
13. Morino, S., Hazama, H., Ozaki, M., Teraoka, Y., Shibata, S., Doi, M., Ueda, H., Ishida, T., and Uesugi, S. (1996) Analysis of the mRNA cap-binding ability of human eukaryotic initiation factor-4E by use of recombinant wild-type and mutant forms. *Eur. J. Biochem.* **239**, 597–601
14. Youtani, T., Tomoo, K., Ishida, T., Miyoshi, H., and Miura, K. (2000) Regulation of human eIF4E by 4E-BP1: binding analysis using surface plasmon resonance. *IUBMB Life* **49**, 27–31
15. Jorgensen, W.L., Chandrasekhar, J., Rico, M., Santoro, J., and Klein, M.L. (1983) Comparison of simple functions for simulating liquid water. *J. Chem. Phys.* **79**, 926–935
16. Cornell, W.D., Cieplak, P., Bayly, C.I., Gould, I.R., Merz, K.M., Jr., Ferguson, D,M,, Spellmeyer, D.C., Fox, T., Caldwell, J.W., and Kollman, P.A. (1995) A second generation force field for the simulations of proteins, nucleic acids, and organic molecules. *J. Am. Chem. Soc.* **117**, 5179–5197
17. Case, D.A., Pearlman, D.A., Caldwell, J.W., Cheatham, III T.E., Ross, W.S., Simmerling, C.L., Darden, T.A., Merz, K.M., Stanton, R.V., Cheng, A.L., Vincent, J.J., Crowley, M., Tsui, V., Radmer, R.J., Duan, Y., Pitera, J., Massova, I., Seibel, G.L., Singh, U.C., Weiner, P.K., and Kollman, P.A. (1999) AMBER 6, University of California, San Francisco
18. York, D., Wlodawer, A., Pedersen, L.G., and Darden, T.A. (1994) Atomic-level accuracy in simulations of large protein crystals. *Proc. Natl. Acad. Sci. USA* **91**, 8715–8718
19. Berendsen, H.J.C., Postma, J.P.M., Van Gunsteren, W.F., DiNola, A., and Haak, J.R. (1984) Molecular dynamics with coupling to an external bath. *J. Chem. Phys.* **81**, 3684–3690
20. Rychaert, J.P., Ciccotti, G., and Berendsen, H.J.C. (1977) Numerical integration of the Cartesian equations of motion of a system with constraints: molecular dynamics of n-alkanes. *J. Comput. Phys.* **23**, 327–341
21. Niedzwiecka, A., Marcotrigiano, J., Stepinski, J., Jankowska-Anyszka, M., Wyslouch-Cieszynska, A., Dadlez, M., Gingras, A.C., Mak, P., Darzynkiewicz, E., Sonenberg, N., Burley, S.K., and Stolarski, R. (2002) Biophysical studies of eIF4E cap-binding protein: recognition of mRNA 5′ cap structure and synthetic fragments of eIF4G and 4E-BP1 proteins. *J. Mol. Biol.* **319**, 615–635
22. Gingras, A.C., Raught, B., Gygi, S.P., Niedzwiecka, A., Miron, M., Burley, S.K., Polakiewicz, R.D., Wyslouch-Cieszynska, A., Aebersold, R., and Sonenberg, N. (2001) Hierarchical phosphorylation of the translation inhibitor 4E-BP1. *Genes Dev.* **15**, 2852–2864
23. Sunaga, A., Kiyatkin, A.B., Hatakeyama, M., Futatsugi, N., Okimoto, N., Hirano, Y., Narumi, T., Kawai, A., Susukita, R., Koishi, T., Furusawa, H., Yasuoka, K., Takada, N., Ohno, Y., Taiji, M., Ebisuzaki, T., Hoek, J.B., Konagaya, A., and Kholodenko, B.N. (2004) Tyr-317 phosphorylation increases Shc structural rigidity and reduces coupling of domain motions remote from the phosphorylation site as revealed by molecular dynamics simulations. *J. Biol. Chem.* **279**, 4657–4662